Epithelioid GBMs Show a High Percentage of *BRAF* V600E Mutation

Bette Kay Kleinschmidt-DeMasters, MD,†‡ Dara L. Aisner, MD, PhD,* Diane K. Birks, MS,†§ and Nicholas K. Foreman, MD§*

Abstract: *BRAF* V600E mutation has been identified in up to 2/3 of pleomorphic xanthoastrocytomas (PXAs), World Health Organization grade II, as well as in varying percentages of PXAs with anaplastic features (PXA-A), gangliogliomas, extracerebellar pilocytic astrocytomas, and, rarely, giant cell glioblastoma multiforme (GC-GBMs). GC-GBMs and epithelioid GBMs (E-GBMs) can be histologically challenging to distinguish from PXA-A. We undertook this study specifically to address whether these 2 tumor types also showed the mutation. We tested our originally reported cohort of 8 E-GBMs and 2 rhabdoid GBMs (R-GBM) as well as 5 new E-GBMs (1 pediatric, 4 adult) and 9 GC-GBMs (2 pediatric, 7 adult) (n = 24) for *BRAF* V600E mutational status. Twenty-one of 24 had sufficient material for IDH-1 immunostaining, which is usually absent in PXAs, PXA-As, and primary GBMs but present in secondary GBMs. Patients ranged in age from 4 to 67 years. *BRAF* V600E mutation was identified in 7/13 of E-GBMs, including 3 of our original cases; patients with mutation were aged 10 to 50 years. None of the 9 GC-GBMs or 2 R-GBMs manifested this mutation, including pediatric patients. The sole secondary E-GBM was the single case manifesting positive IDH-1 immunoreactivity. A high percentage of E-GBMs manifest *BRAF* V600E mutation, paralleling PXAs. All R-GBMs and GC-GBMs were negative, although larger multi-institutional cohorts will have to be tested to extend this result. *BRAF* V600E mutational analyses should be performed on E-GBMs, particularly in all pediatric and young-aged adults, given the potential for *BRAF* inhibitor therapy in this subset of GBM patients.

Key Words: giant cell GBM, epithelioid GBM, pleomorphic xanthoastrocytoma, *BRAF*, IDH-1, ganglioglioma

(*Am J Surg Pathol* 2013;37:685–698)

From the Departments of *Pathology; †Neurosurgery; ‡Neurology, The University of Colorado Health Sciences Center; and §Department of Neuro oncology, Children's Hospital Colorado, Aurora, CO.

Accepted for abstract presentation at the 52nd annual meeting of the Canadian Association of Neuropathologists, October 24th to 27th, Mont-Tremblant, QC, Canada.

Conflicts of Interest and Source of Funding: Financially supported by the Morgan Adams Foundation. The authors have disclosed that they have no significant relationships with, or financial interest in, any commercial companies pertaining to this article.

Correspondence: Betty Kay Kleinschmidt-DeMasters, MD, 12605 E. 16th Avenue, Room 3026, MS F768, Aurora, CO 80045 (e-mail: bk.demasters@ucdenver.edu).

Mutation in *BRAF* V600E at position 600, specifically V600E (NM_004333.4 c.1799 T > A, hereafter referred to as *BRAF* V600E), has been identified as a common finding in certain central nervous system tumors, most notably in pleomorphic xanthoastrocytomas (PXAs) (World Health Organization [WHO] grade II) and PXA with anaplastic features (PXA-As), as well as in fewer numbers of gangliogliomas, extracerebellar pilocytic astrocytomas, and, rarely, giant cell glioblastoma multiforme (GC-GBMs).[1–3] Because of the infrequency with which this mutation is seen in diffuse astrocytic tumors WHO grades II, III, and IV,[3] it has been suggested that the presence of *BRAF* V600E may be helpful in distinguishing PXAs from histologic mimics.[2] An unresolved issue, however, is whether the age of the patient may affect the percentage of tumors that are positive for this mutation. Schindler et al[3] found that 38% of adult PXA-As showed this mutation, compared with 100% of pediatric PXA-As.

In contrast, a common mutation in isocitrate dehydrogenase 1 (*IDH-1*) is typical of the majority of diffuse astrocytomas, oligodendrogliomas, and mixed oligoastrocytomas of WHO grades II and III, as well as secondary GBMs.[4,5] Primary GBMs almost never show mutation in *IDH-1*, and PXAs, PXA-As, gangliogliomas, and pilocytic astrocytomas are also almost always negative for *IDH-1* mutation.[4] Immunohistochemical (IHC) staining for IDH-1 correlates strongly with the *IDH-1* mutational status as assessed by polymerase chain reaction (PCR) testing[6] and thus can serve as a cost-effective and time-effective substitute for full mutational analysis assessment.

Among the most challenging histologic tumor types to diagnose is the PXA-A. PXA is a rare WHO grade II tumor, first fully characterized by Kepes et al,[7] which demonstrates a *relatively* favorable clinical course.[7–10] PXA-A designates a subset that may show a more aggressive clinical course but has yet to be assigned a formal WHO grade.[10] Both PXAs and PXA-As are more common in children and young adults,[7,9,10] but well-documented cases have been seen in patients 40 years or older.[11–16] PXA-A may arise de novo[17,18] or may develop anaplastic features after recurrence of a previous WHO grade II PXA.[12,14,17–23] Recent reviews by Tekkök et al,[21] Okazaki et al,[22] and Vu et al[23] underscore the fact that for either de novo PXA-As or PXA-As that secondarily transform from PXA WHO grade II, prognosis is often, but not invariably, poor.

Whereas PXA, WHO grade II, is unlikely to be mistaken for a GBM, PXA-As (a tumor more akin to WHO grade III) and GBMs (WHO grade IV) both share high-grade features such as increased mitotic activity and often necrosis. The WHO 2007 fascicle suggests that mitotic activity of ≥ 5 mitoses per 10 high-power fields best correlates with adverse prognosis in PXA and thus should yield PXA-A diagnosis.[10] Necrosis also adversely affects survival[9,24–26] and is frequently present in PXA-A. Most GBMs lack sufficient nuclear pleomorphism, cytoplasmic lipidization, reticulin-rich areas, or lymphocytic infiltrates[27] to cause diagnostic confusion with PXA-A for the pathologist. The exceptions to this, however, are 2 GBM subtypes: GC-GBM and epithelioid GBM (E-GBM).

GC-GBM is a well-described variant in the WHO 2007 fascicle, which manifests bizarre multinucleated giant cells, abundant reticulin investiture, often prominent lymphocytic infiltrates and cytoplasmic lipidization,[27] and can be challenging to distinguish from PXA-A.[28] Genetically, GC-GBMs typically lack the *EGFR* amplification/overexpression of primary GBMs, but, like primary GBMs, approximately the same percentage (33%) share *PTEN* mutation. Up to 84% have *TP53* mutation, a rate more parallel to secondary than primary GBMs.[27] Although *TP53* mutational status is often not assessed in routine practice, positive *TP53* mutational status can correlate with strong p53 nuclear IHC expression in glial tumors.[29]

E-GBM is even rarer than GC-GBM and is not a formal variant in the 2007 WHO fascicle. E-GBMs are composed of cohesive sheets of patternless, closely packed, variably lipidized, small-sized to medium-sized cells with rounded cytoplasmic profiles, eosinophilic cytoplasm, lack of cytoplasmic stellate processes, and absence of interspersed neuropil.[30–36] Tumors may additionally possess rich reticulin investiture but, unlike PXA-As, usually possess more cytologically uniform cells and an absence of eosinophilic granular bodies.[35]

In the current study, we tested the hypothesis that E-GBMs or GC-GBMs might possess the *BRAF* V600E mutation. Given the rarity of these subtypes of GBMs, we reinterrogated our originally published cohort of 8 E-GBMs and 2 rhabdoid GBMs (R-GBMs)[35] as well as 5 new E-GBM cases and 9 GC-GBMs from our files. The results of this report support our hypothesis that a significant percentage of E-GBMs, particularly (but not exclusively) those in young adults and children, share the *BRAF* V600E genetic background of PXA, PXA-A, ganglioglioma, and extracerebellar pilocytic astrocytoma. In contrast, we were unable to identify the mutation in GC-GBMs or R-GBMs.

MATERIALS AND METHODS

Case Accrual

Institutional research review board approval was obtained for this study. Cases were identified by diagnosis from our pathology department databank and/or personal files of the authors for the years 2000 to 2011, inclusive, for E-GBMs and R-GBMs. Designations of E-GBM and R-GBM had not been utilized in our system before 2000 and thus were not retrievable by text word search of our databases before 2000. However, GC-GBMs have existed as separate entities for a considerably longer time period and thus could be identified from the year 1994 to the present.

All slides were rereviewed for diagnosis confirmation by the senior neuropathologist on the study (B.K.K.-D.); only cases in which a predominant (> 30% to 40%) tumor component manifested the E-GBM, R-GBM, or GC-GBM feature were utilized for this study. Cases in which slides or paraffin blocks were no longer available were excluded from the study.

In all examples, efforts were made to exclude the histologic diagnosis of PXA-A. Criteria for diagnosis of PXA-A were applied, as detailed by Giannini et al.[9,10] As noted by Giannini and colleagues, "although it was not stressed in the original description of PXA or in the WHO monograph, granular bodies of varying size, texture, and eosinophilia are a regular feature of this tumor (ie, PXA-A)."[9] In our own experience, the presence of multiple granular bodies, particularly the eosinophilic refractile type, within a tumor has been the single most helpful clue to diagnosis of PXA. None of our E-GBMs, GC-GBMs, or R-GBMs possessed multiple eosinophilic granular bodies. None possessed areas of classic low-grade PXA juxtaposed to high-grade glioma, as has previously been described in cases of PXA-A.[7,25]

Neuroimaging disks and original neuroimaging reports were available for review on all new E-GBM cases. Several of these patients were first seen for histologic review of slides and diagnosis, after which the patients were referred to our tertiary center for treatment considerations. Thus, additional neuroradiology interpretation from neuroradiologists within our system allowed comparisons between outside and in-house neuroimaging impressions.

Survival data had been recorded in our original cohort of 2 R-GBM and 8 E-GBM patients recorded in that manuscript.[35] Follow-up information was sought in those known to be living at the time of that report. Survival was also investigated in all patients in whom the diagnosis had been made before 2009. However, the short (< 3 y) interval between diagnosis and this report for new E-GBM and several GC-GBM cases made survival information for these more recently diagnosed patients less meaningful. In cases in which survival data could be obtained, however, this was anecdotally noted, with survival recorded as of June 1, 2012.

Methods for Histology

For light microscopy, tumor sections were cut at 4 μm and stained with hematoxylin and eosin. IHC analysis for glial fibrillary acidic protein (GFAP; Dako, Carpinteria, CA; monoclonal; 1:100 dilution) and TP53 (Dako; monoclonal; 1:200 dilution) was performed on the

entire cohort, with synaptophysin (Ventana, Tucson, AZ; polyclonal; predilute), neurofilament (Ventana; monoclonal; predilute), and BAF47 (INI-1 protein; BD Transduction; monoclonal; 1:250 dilution) immunostaining conducted additionally on all E-GBMs.

The immunostaining pattern for INI-1 was recorded as retained or lost in all nuclei or in a subset of tumor nuclei. The IHC result for IDH-1 (Dianova HistoBio, Miami Beach, FL; clone H09; monoclonal; 1:40 dilution) was recorded as positive or negative in tumor cell cytoplasm. p53 immunostaining was estimated semiquantitatively, with a score of 0 given for $<1\%$, 1+ for 1% to 5%, 2+ for 6% to 25%, 3+ for 26% to 50%, and 4+ for $>50\%$ of tumor cells showing immunoreactivity; TP53 immunostaining was conducted on E-GBMs as performed in the study by Rodriguez et al.[33] Efforts were made to exclude nontumoral vascular, stromal cells and hematopoietic cells in the semiquantitative estimates.

IHC analysis for IDH-1 was performed on all cases except 3 instances in which insufficient tissue remained (cases 2, 5, 9; Table 1). IDH-1 IHC was of a uniform pattern throughout the tumor and was either positively expressed in the cytoplasm of all tumor cells or negative in all tumor cells.

Scoring for IHC Features for All Tumors With *BRAF* Mutation

Paralleling our original study on E-GBMs, scoring of *extent/severity* of necrosis, lymphocytes, and reticulin fibers between individual or small groups of tumor cells was assessed using the Gomori reticulin stain. Presence or absence of synaptophysin or neurofilament immunostaining was assessed. Scoring for these features was performed as in our previous study.[35]

Necrosis was semiquantitatively assessed on a 0 to 3+ scale, with 0 indicating no necrosis present on the biopsy/resection specimen, 1+ indicating focal small areas of necrosis, and 2+ indicating presence of multifocal broad zones of necrosis or pseudopalisading necrosis. A score of 3+ was reserved for cases with extensive necrosis, estimated to occupy 10% or more of the sampled specimen. Inflammation (lymphocytes) within the tumors was scored as absent (0), focally present (1+), or prominent (2+). Reticulin fiber deposition between individual or small groups of tumor cells was assessed using the Gomori reticulin stain and recorded as being absent (0), focally present (1+), or focally prominent (2+) between tumor cells. In cases in which this change was focally present, it was noted as such. Immunostaining for synaptophysin and neurofilament was recorded as being absent (0) or focally present (1+).

Methods for Fluorescence In Situ Hybridization

Fluorescence in situ hybridization (FISH) had been conducted as part of the routine workup at the time of diagnosis in most cases. Briefly, dual-color FISH probe sets, manufactured by Vysis (Abbott Laboratories Inc., Des Plaines, IL), were used for loss of heterozygosity studies of chromosomes 1p36 and 19q13 and amplification status of *EGFR*. The probe sets were: chromosomes 1p36 (Spectrum Orange) and 1q25 (Spectrum Green); chromosomes 19p13 (Spectrum Green) and 19q13 (Spectrum Orange); EGFR (7p12-Spectrum Orange) and CEP7 (D7Z1-Spectrum Green). To test for monosomy 22, DNA probes directed to 22q11.2 and 22q13 were used; this method detects most deletions but does not detect point mutations in chromosome 22. For analysis of PTEN, a *PTEN* (10q23)-specific DNA probe and a probe directed to the chromosome 10 centromere were used.

Methods for V600E *BRAF* Mutational Analyses

Most cases had unstained slides available for microdissection by 1 of the authors (D.L.A.), although in several instances immunonegative slides prepared at the time of original diagnosis remained the only available material for microdissection. Tumor tissues with epithelioid, rhabdoid, or giant cell morphology were specifically identified, circled by the neuropathologist (B.K.K.-D.), and targeted for microdissection and assessment. In 2 pediatric cases, tumor DNA prepared from frozen tissue obtained at the time of surgical excision was additionally available for mutational testing (cases 16 and 17, both pediatric GC-GBMs). Thus, 2 samples could be tested from 2 differing areas of the tumor for *BRAF* V600E; that is, from tumor DNA and from microdissection paraffin-scraped material.

In the case of the material microdissected from slides, paraffin sections were thoroughly deparaffinized in xylene, hydrated through graded alcohols to water, and stained with Gill hematoxylin. Slides were covered with glycerol to prevent cell dispersion and isolated under a dissecting microscope using a scalpel point or a hollow borosilicate glass pipette. The scraped material was washed in phosphate-buffered saline and digested in proteinase K overnight at 37°C in ATL Buffer (Qiagen Inc.). DNA was then isolated using QIAamp DNA FFPE extraction kit (cat # 56404) according to manufacturer instructions.

In the case of paraffin tissue blocks (1 case), paraffin scrolls were deparaffinized in xylene as above, followed by reconstitution in graded alcohols and phosphate-buffered saline and treated in a parallel manner. DNA yields were then quantified using a Nanodrop spectrophotometer ND-1000 (Thermo Fisher Scientific Inc., Waltham, MA).

For direct sequencing, approximately 10 ng of template DNA was PCR amplified using 5 pmol each of forward (5′TGCTTGCTCTGATAGGAAAAT3′) and reverse (5′TCAGGGCCAAAAATTTAATCA3′) *BRAF* exon 15 primers KAPA2G Robust HotStart Enzyme and PCR master mix with KAPA dNTP mix (KAPA Biosystems; cat# KK5525 and KK1017) in a 25 μL reaction mix. PCR was performed on an ABI 9700 thermocycler with an initial denaturing step at 95°C, followed by 20 cycles of touchdown PCR (starting annealing temperature of 65°C, decremented by 0.5°C per cycle) and 25 cycles of denaturation at 94°C, annealing at 55°C, and extension at 72°C, and finished by a final extension at 72°C for 10 minute. The resultant PCR products were purified with the QIAquick 96-well PCR cleanup kit

TABLE 1. Clinical, Immunohistochemical, Molecular, and Cytogenetic Features

Patient Age Sex Year of Surgical Biopsy/ Resection Tumor Location Surgical Procedure	Diagnosis	*BRAF* V600E Mutational Status	BAF47 (INI-1) IHC	FISH for EGFR, PTEN, Monosomy 22, LOH 1p, 19q	p53; *IDH-1* IHC	Clinical Outcome/ Interval to Demise or Survival
R-GBMS						
1 18 M 1999 Right frontal Resection	Primary R-GBM	No mutation present	BAF47 Focally lost in nuclei of rhabdoid cells, but not in nonrhabdoid areas	Negative for EGFR amplification Monosomy 22 demonstrated on culture as minor clone	p53 1+ *IDH-1* negative	Died 22 wk Autopsy showed residual tumor in right frontal lobe, adjacent leptomeninges Implantation metastasis in right frontoparietal scalp, microscopic metastases in both lungs
2 67 F 2007 C Right occipital lobe Resection	Primary R-GBM	No mutation present	BAF47 Focally lost in nuclei of rhabdoid cells, but not in nonrhabdoid areas	Positive for high-level amplification EGFR Positive for loss of PTEN (10q23) sequences Positive for loss of 22q11.2 and 22q13 sequences, consistent with monosomy 22 (genetic findings present in both histologically rhabdoid and nonrhabdoid areas)	p53 2+ *IDH-1* not tested due to inadequate tissue	Died 36 wk
E-GBMS						
3 24 M 1997 C 1997 (2 surgical procedures same year) Right temporal Biopsy Resection	Primary E-GBM	No mutation present	BAF47 Retained in all tumor nuclei	Negative for EGFR amplification	p53 2+ *IDH-1* negative	Developed cerebrospinal fluid dissemination (+CSF cytology) Died 25 wk
4 27 F 2001 Left occipital Resection	Primary E-GBM	V600E mutation present	BAF47 Retained in all tumor nuclei	Positive for cells with EGFR amplification	p53 4+ *IDH-1* negative	Alive as of May 1, 2008 328 wk
5 18 M 2002 C Right frontoparietal Resection	Primary E-GBM Patient with lower limb amputation for developmental anomaly, recurrent Burkitt lymphoma of gastrointestinal tract Known germline short-arm chromosome 22 abnormality	No mutation present	BAF47 Retained in all tumor nuclei	Negative for EGFR amplification	p53 4+ *IDH-1* not tested because of inadequate tissue	Alive as of March 31, 2009 267 wk Lost to follow-up after 2009
6 25 M 2003 C Cerebellar hemisphere Resection	Primary E-GBM	No mutation present	BAF47 Retained in all tumor nuclei	Negative for monosomy of Ch. 22	p53 4+ *IDH-1* negative	Died 66 wk

TABLE 1. (*continued*)

	Patient Age Sex Year of Surgical Biopsy/ Resection Tumor Location Surgical Procedure	Diagnosis	*BRAF* V600E Mutational Status	BAF47 (INI-1) IHC	FISH for EGFR, PTEN, Monosomy 22, LOH 1p, 19q	p53; *IDH-1* IHC	Clinical Outcome/ Interval to Demise or Survival
7	43 M 2003 C Left temporal-Parietal Resection	Primary E-GBM	V600E mutation present	BAF47 Retained in all tumor nuclei	Negative for monosomy of Ch. 22	p53 1+ *IDH-1* negative	Died October 23, 2003 26 wk
8	41 M 2003 Right frontal Resection	Secondary E-GBM arising as a well-demarcated enhancing mass in cavity of previous surgical resection bed Previous mixed oligoastrocytoma, WHO grade II, 2 y prior	No mutation present	BAF47 Retained in all tumor nuclei	Negative for monosomy of Ch. 22 Negative for LOH 1p, 19q (testing performed on E-GBM)	p53 4+ *IDH-1* positive	Alive as of August 1, 2009 306 wk Alive as of June 1, 2012
9	69 M 2007 C Left frontal lobe Biopsy	Primary E-GBM	No mutation present	Not tested due to inadequate tissue	Not tested	p53 not tested due to inadequate tissue *IDH-1* not tested due to inadequate tissue	Died 85 wk
10	10 F 2009 2009 (2 surgical procedures same year) Right parieto-occipital Biopsy Resection	Primary E-GBM	V600E mutation present	BAF47 Retained in all tumor nuclei	Negative for EGFR amplification Negative for loss of PTEN (10q23) sequences Negative for monosomy of Ch. 22	p53 2+ *IDH-1* negative	Alive as of August 1, 2009 24 wk Alive as of June 1, 2012
11	29 M 2012 Left temporal lobe Resection	Primary E-GBM	V600E mutation present	BAF47 Retained in all tumor nuclei	Negative for EGFR amplification Low-level loss of PTEN and 10 centromere consistent with monosomy 10 Negative for monosomy of Ch. 22	p53 1+ *IDH-1* negative	Alive as of June 1, 2012
12	21 F 2012 C Right temporal lobe Resection	Primary E-GBM	V600E mutation present	BAF47 Retained in all tumor nuclei	Negative for amplification of EGFR sequences Negative for loss of PTEN sequences Weak EGFR expression	p53 1+ *IDH-1* negative	Alive as of June 1, 2012
13	14 M 2011 Right frontal lobe Biopsy	Primary E-GBM	No mutation present	BAF47 Retained in all tumor nuclei	Rare cells with amplification of EGFR (1.8%); other cells with polysomy (3-4, 43.6%), and high polysomy for Ch. 7 (≥ 5, 35.0%) Borderline for loss of PTEN and 10 centromere, suggesting monosomy 10 Negative for monosomy of Ch. 22	p53 0 *IDH-1* negative	Alive as of June 1, 2012

TABLE 1. (*continued*)

	Patient Age Sex Year of Surgical Biopsy/ Resection Tumor Location Surgical Procedure	Diagnosis	*BRAF* V600E Mutational Status	BAF47 (INI-1) IHC	FISH for EGFR, PTEN, Monosomy 22, LOH 1p, 19q	p53; *IDH-1* IHC	Clinical Outcome/ Interval to Demise or Survival
14	29 F 2012 C Left temporal-parietal lobe Resection	Primary E-GBM	V600E mutation present	BAF47 Retained in tumor nuclei	Negative for amplification of EGFR sequences Positive for loss of PTEN and 10 centromere sequences, consistent with monosomy 10	p53 2+ *IDH-1* negative	Alive as of June 1, 2012
15	50 M 2012 Left temporal lobe Resection C	Primary E-GBM	V600E mutation present	BAF47 Retained in tumor nuclei	Negative for amplification of EGFR sequences Positive for loss of PTEN and 10 centromere sequences, consistent with monosomy 10	p53 1+ *IDH-1* negative	Alive as of June 1, 2012
GC-GBMS							
16	4 F 2008 (2 surgical procedures same year) 2009 Right temporal lobe Resection	Primary GBM, giant cell variant	No mutation present	Not tested	Not tested	p53 1+ *IDH-1* negative	Alive as of June 1, 2012
17	14 F 2002 (2 surgical procedures same year) Biopsy Resection	Primary GBM, giant cell variant	No mutation present	Not tested	Not tested	p53 4+ *IDH-1* negative	Died 72 wk
18	47 M 2008 (biopsied 2007, misdiagnosed as metastatic sarcoma, given stereotactic radiosurgery; on review GC-GBM) Previous maxillary sinus osteosarcoma resected 2001 Right occipital lobe Resection	Primary GBM, giant cell variant	No mutation present	Not tested	Positive for gain of chromosome 7 Positive for loss of chromosome 10 (including PTEN) Negative for amplification of EGFR (7p12)	p53 4+ *IDH-1* negative	Alive as of June 1, 2012*
19	69 F 2002 Parieto occipital lobe (side unspecified) Resection	Primary GBM, giant cell variant	No mutation present	Not tested	Not tested	p53 3+ *IDH-1* negative	Died 66 wk
20	45 F 2000 2005 Left temporal lobe Resections	Primary GBM, giant cell variant	No mutation present	Not tested	No evidence of amplification of EGFR (7p12) sequences Negative for deletion of 1p36 sequences (ratio 1p36:1q25 = 1.06) Negative for deletion of 19q13 sequences (ratio 19q13:19p13 = 1.11)	p53 0 *IDH-1* negative	Alive as of June 1, 2012
21	31 M Left frontal lobe Resection	Primary GBM, giant cell variant	No mutation present	Not tested	Not tested	p53 3+ *IDH-1* negative	Died 47 wk

TABLE 1. (*continued*)

	Patient Age Sex Year of Surgical Biopsy/ Resection Tumor Location Surgical Procedure	Diagnosis	*BRAF* V600E Mutational Status	BAF47 (INI-1) IHC	FISH for EGFR, PTEN, Monosomy 22, LOH 1p, 19q	p53; *IDH-1* IHC	Clinical Outcome/ Interval to Demise or Survival
22	60 F 2012 2011 2008 dx'd as grade III astrocytoma, outside hospital Right frontal lobe Resection	Secondary GBM, giant cell variant	No mutation present	Not tested	Positive for amplification of EGFR sequences Negative for loss of PTEN sequences	p53 4+ *IDH-1* negative	Alive as of June 1, 2012
23	50 F 2010 2008, dx'd as GBM, outside hospital Right parietal lobe Resection	Primary GBM, giant cell variant	No mutation present	Not tested	Negative for deletion of 1p36 sequences (ratio p36:1q25 = 0.93) Negative for deletion of 19q13 sequences (ratio 19q13:19p13 = 0.92) Positive for amplification of EGFR sequences Positive for loss of PTEN and 10 centromere, consistent with monosomy 10	p53 0 *IDH-1* negative	Alive as of June 1, 2012
24	63 M 1998 Left posterior frontal lobe Biopsy	Primary GBM, giant cell variant	No mutation present	Not tested	Not tested	p53 0 *IDH-1* negative	Died 64 wk

Case 4 was seen in consultation by neuropathologists at Mayo Clinic, Duke, and Johns Hopkins; diagnoses were GBM with epithelioid features (consultant notes that "no definite pleomorphic xanthoastrocytoma component is present"); GBM with abundant reticulin; malignant glioma with features of E-GBM.

Case 8 was seen at Duke before entering a treatment protocol and diagnosed as GBM.

Case 18 maxillary sinus lesion seen in consultation by soft tissue pathologist at Massachusetts General Hospital and diagnosed as osteosarcoma, chondroblastic type, grade 2 of 3.

IHC scoring for p53: 0 (< 1%), 1+ (1% to 5% cells immunoreactive); 2+ (6% to 25% immunoreactive); 3+ (26% to 50% immunoreactive); 4+ (> 50% cells immunoreactive).

*This patient was alive at the study closure date but succumbed in September 2012.

C indicates consultation case; Ch indicates chromosome; CSF, cerebrospinal fluid; F, female; LOH, loss of heterozygosity; M, male; ND, not done.

(Qiagen; cat# 28106). The purified PCR products were sequenced in forward and reverse directions using an ABI 3730 automated sequencer using BigDye Terminator Version 1.1 (Applied Biosystems). Each chromatogram was visually inspected for any abnormalities, using NM_004333.4 as a reference sequence, with particular attention directed to codon 600. Sequences were also evaluated using Mutation Surveyor software (Soft Genetics, State College, PA). Mutations were determined to be present when peaks reached a threshold value above baseline calculated from the background level, combined with visual inspection of the chromatogram.

RESULTS

Demographic Features of the Cohort

Demographic, clinical, treatment, and histologic features are detailed in Table 1. A total of 24 patients were studied (11 female, 13 male). Patients ranged in age from 4 to 67 years for the entire cohort, with the 2 R-GBMs from patients aged 18 and 67 years.[35] No additional, new examples of R-GBMs were identified for inclusion. Of the total 13 E-GBMs, 5 represented new cases since our original study—that is, these patients were newly diagnosed since 2009, and of these, 3 were consultation cases (Table 1). Within the E-GBM cohort (n = 13), patient ages ranged from 10 to 69 years, with 9/13 patients being less than 30 years of age. Three of these patients were pediatric, as defined by ages 18 years or less at the time of diagnosis (cases 5, 10, 13; Table 1). One patient had a past diagnosis of a mixed oligoastrocytoma 2 years antecedent to his E-GBM; this case was recorded as a secondary E-GBM (case 8). The remaining 12 E-GBMs were primary GBMs; that is, they occurred de novo. Of the 9 GC-GBMs, 8 were primary/de novo GBMs and 1 was secondary (case 22). Patients with

GC-GBMs had ages ranging from 4 to 63 years; the 2 pediatric patients were aged 4 and 16 years (cases 16 and 17, respectively).

Survival Features of the Cohort

Although survival data had been calculated for our original E-GBM and R-GBM cohort (35), the follow-up was <3 years (ie, diagnosis made since 2009 or later) for all of our new E-GBMs and thus likely not meaningful. All 5 new E-GBMs were alive at the time of study closure (June 1, 2012). Anecdotally, from our original study, cases 4 (diagnosed in 2001), 8 (diagnosed in 2003 as secondary E-GBM), and 10 (diagnosed in 2009) were also known to be alive as of the study closure date. Patient 5, who was alive at the time of our original report,[35] was lost to follow-up. Both R-GBMs succumbed quickly to their disease and were so reported in our original study.[35] Survival times have been noted in the current manuscript in Table 1.

One of the 2 pediatric patients with GC-GBMs is currently alive (diagnosed in 2008; case 16). Several of the adult GC-GBM patients were also alive as of the study closure date: case 20 (diagnosed in 2000, recurrence in 2005) and case 23 (diagnosed in 2010 and treated on experimental vaccine protocol). Case 18 (diagnosed in 2008) was alive and in hospice as of the study closure date but recently succumbed in September 2012 (after study closure). Numbers were obviously too small to provide meaningful data but suggested that some GC-GBMs also enjoy longer survival times.

Neuroimaging Features of New E-GBMs

Neuroimaging features, where known, had been illustrated in our original cohort (Fig. 1; see Kleinschmidt-DeMasters et al[35]). Neuroimaging information was acquired for all 5 new E-GBMs. All 5 new E-GBM cases showed large tumors with complex cystic and solid enhancing areas (Figs. 1A, F). None showed a simple mural nodule-cyst configuration. Despite the fact that none of the 5 new E-GBMs had a clinical history of an antecedent low-grade glioma (ie, none fit the clinical criteria for secondary E-GBMs), 2 of the 5 original neuroimaging reports we obtained mentioned possible, or definite, bony changes in adjacent skull, suggesting that antecedent low-grade or long-standing tumors had existed before the E-GBM was diagnosed/became clinically obvious (cases 13 and 14). Specifically, the original neuroimaging report on case 13 noted that "the skull over the right frontal lobe is equivocally minimally thinner than the left, with less of a marrow space identified on several images, although this finding is subtle and not definite." Case 14 had a neuroimaging report that noted "mild remodeling of the overlying skull," and this was confirmed by us on review of neuroimaging studies from this consultation case. Case 12 had no mention of bony changes in the original report, but on detailed review here of her studies, after referral to our institution, significant bony changes were identified (Fig. 1D). Case 11 had no bony changes, neither in the original report nor on review.

Retrospective Correlation of *BRAF* Results With Neuroimaging Features of New E-GBMs

After receipt of *BRAF* results, we attempted to correlate the bony changes with the *BRAF* mutational status to see whether this radiologic feature might predict mutational status and preempt the need for mutational analysis. Cases 13 and 14 both had mild skull changes that suggested the possibility of a more long-standing tumor; these cases did and did not, respectively, possess the mutation (see below and Table 1). Case 12 had bony changes only on detailed review; she was positive for the mutation. Case 11 had no bony changes and was negative for the mutation. Thus, on the basis of a very small number of cases, there was no correlation between neuroimaging features of bony thinning or erosion and *BRAF* V600E status. The degree of surrounding edema also varied, with a significant midline shift seen in case 11 (Fig. 1E) but relatively little edema surrounding the tumor in case 15. Hence, the extent of edema was also not predictive of the *BRAF* status for individual patients.

Histologic Features of E-GBMs

Histologic features of E-GBMs and R-GBMs were detailed in our original report.[35] Features of E-GBMs were recapitulated in the 5 new cases and were further illustrated here. E-GBMs were characterized by relatively monotonous sheets of small-sized to moderate-sized epithelioid cells with eosinophilic cytoplasm with rounded cell borders and a paucity of stellate cytoplasmic processes (Figs. 2A, G). At higher-power magnification, prominent nucleoli and abundant eosinophilic cytoplasm could be seen, sometimes mimicking a rhabdoid phenotype (Fig. 2B, arrow). Discohesive tumor cells could lead to areas almost identical to metastatic carcinoma or melanoma (Fig. 2C). Variable numbers of accompanying non-neoplastic lymphocytes (arrow) added to the diagnostic overlap, at least focally, with metastatic carcinoma or melanoma (Fig. 2D). E-GBMs in most cases showed almost complete cellular monotony (cases 11, 12, and 15), although slightly more variation in cellular size and scattered larger, sometimes multinucleated (arrow), cells could be identified, as shown in case 13 (Fig. 2E). Necrosis (arrow) was identified in 4 of 5 new E-GBMs (Figs. 2F, G). Multiple mitotic figures (arrows) were found in all examples (Fig. 2G). Strong diffuse S100 immunoreactivity (top) with more variable and patchy GFAP immunostaining (bottom) was typical of E-GBMs (Fig. 2H). In 1 case (case 14), focal spindled morphology of some cells was highlighted by GFAP (Fig. 2H, arrows). Increased reticulin fiber deposition could be found in E-GBMs, but was often quite focal (Fig. 2I).

In terms of the *extent* of these features, necrosis was extensive in cases 11 and 12 (scored as 3+), moderate in cases 13 and 14 (scored as 2+), and absent in case 15 (scored as 0), which had focal microvascular proliferation to meet WHO GBM criteria. Lymphocytic collections were absent in 1 case (case 13), focally present in cases 11 and 14 (scored as 1+), and focally prominent in cases 12 and 15 (scored as 2+). Reticulin fiber deposition between

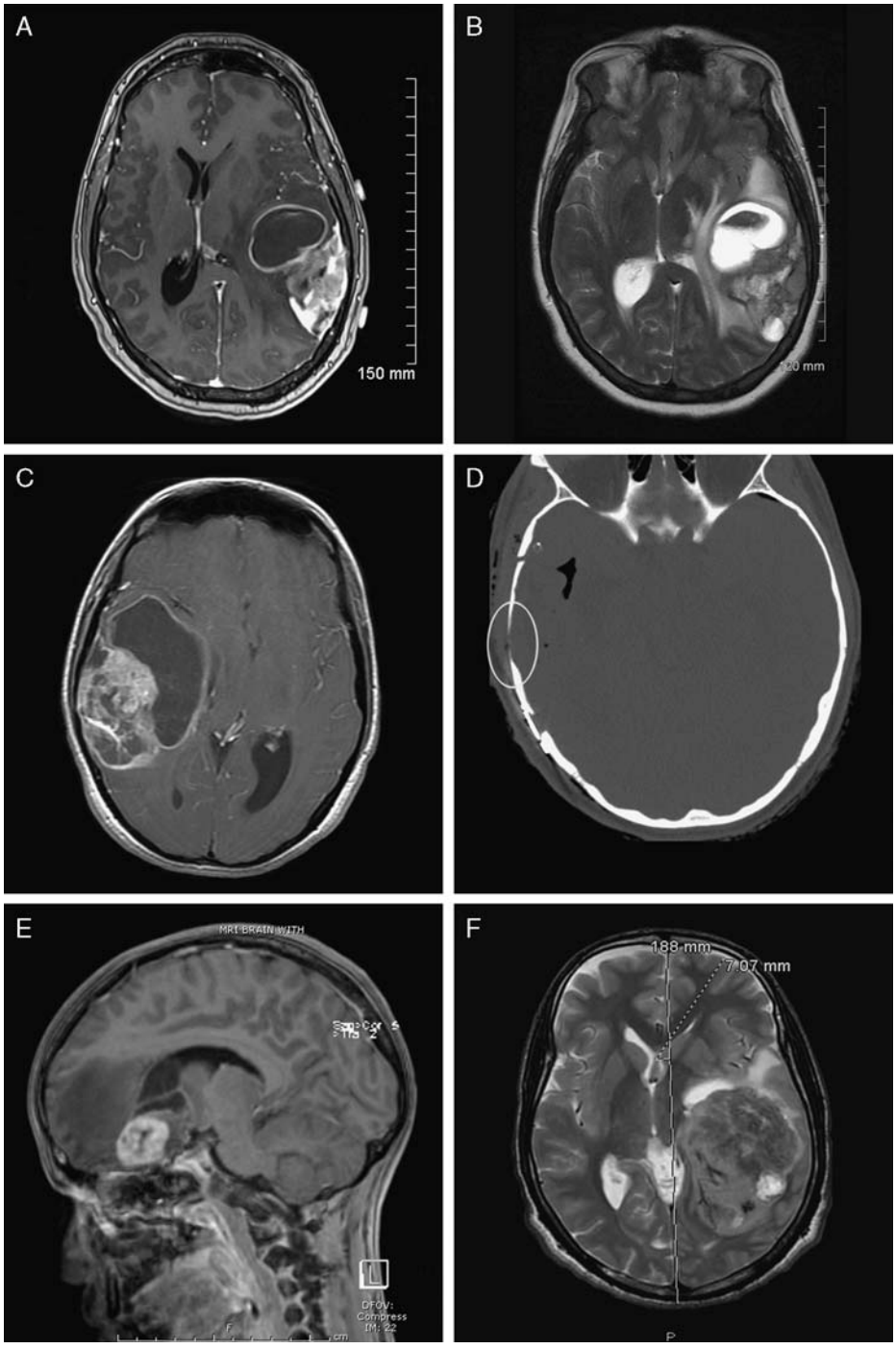

FIGURE 1. A, Magnetic resonance imaging (MRI) scan, axial, T1-weighted scan with gadolinium enhancement, shows an E-GBM with complex cystic and solid enhancing areas; none of the 5 new E-GBM cases in this study showed a simple mural nodule-cyst configuration (case 14 illustrated). B, MRI scan, axial, T2-weighted, better highlights the bright signal in the cystic portions of this same E-GBM, as well as the surrounding edema and midline shift generated by this high-grade tumor (case 14 illustrated). C, MRI scan, axial, T1-weighted with gadolinium, from another E-GBM shows an even larger cystic component in this example (case 12 illustrated). D, Computerized tomographic scan, axial, shows the nearby bony thinning (encircled) in this same patient, suggesting that a more long-standing tumor had been present. Despite this radiographic feature, low-grade tumor areas were not identified in the resection specimen (case 12 illustrated). E, MRI scan, sagittal, T1-weighted with gadolinium, shows a small cystic component and more solid, relatively well-demarcated enhancing component in this pediatric patient with E-GBM; note the significant surrounding edema (dark intensity signal) (case 13 illustrated). F, MRI scan, axial, T2-weighted, highlights the massive size of some of these E-GBMs, as measured on the scan, as well as the extent of midline shift that can be produced (case 11 illustrated).

individual or small groups of tumor cells as assessed using the Gomori reticulum stain was recorded as being absent in case 12 (scored as 0), focally present in case 11 (scored as 1+), or focally prominent in cases 13, 14, and 15 (scored as 2+).

IHC Features of E-GBMs

Synaptophysin immunoreactivity was identified in rare cells (scored as 1+) only in cases 12 and 15, with rare cells immunoreactive for neurofilament only in cases 12 and 14 (scored as 1+). Thus, the current cohort extended

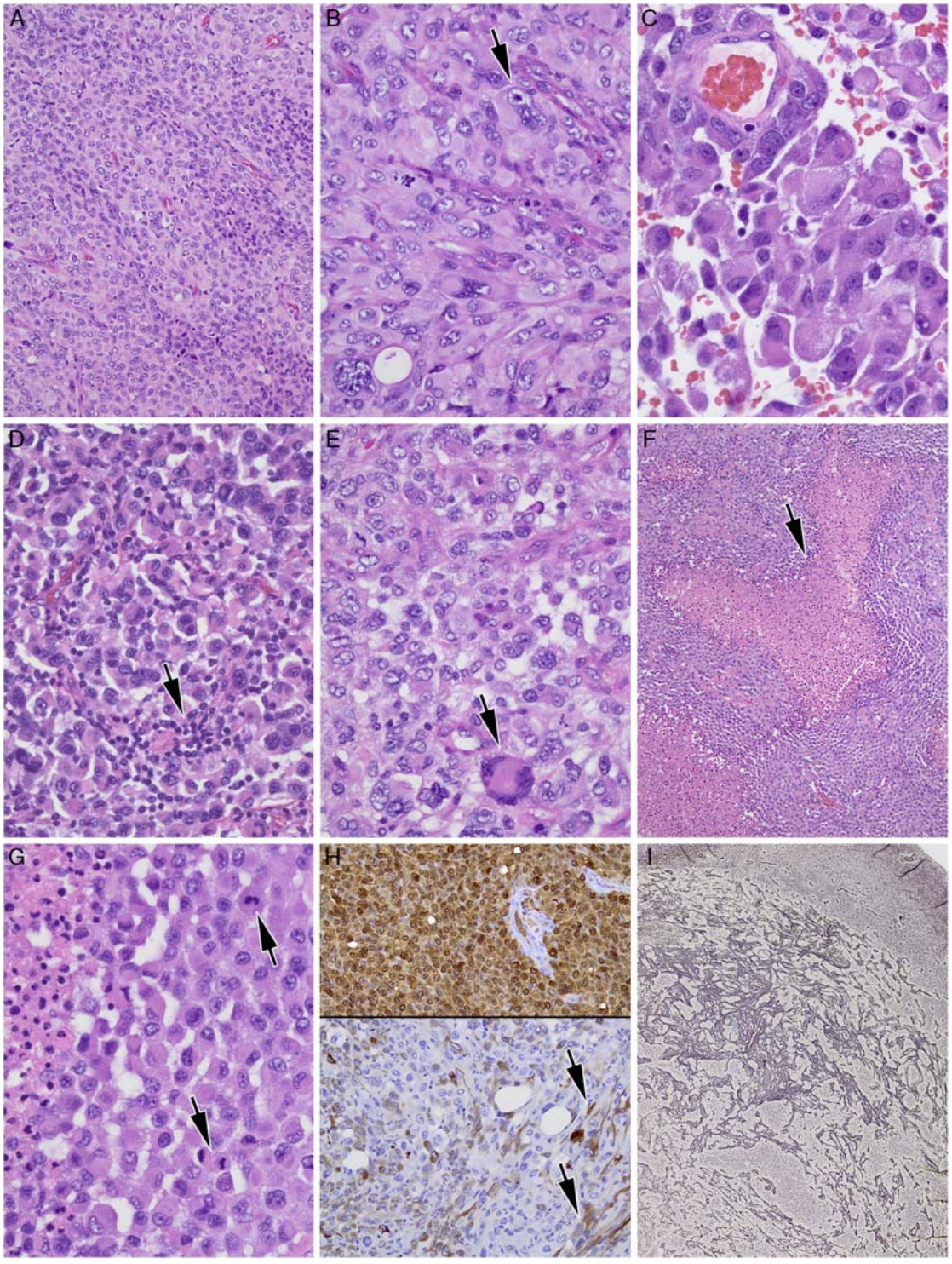

our previous findings[35] that necrosis, lymphocytic collections, increased reticulin fiber deposition, and occasionally rare cells immunoreactive for neuronal markers were features of many E-GBMs, although all features were not found in all tumors.

Four of our 12 assessable E-GBMs showed strong (ie, 3+ or 4+) immunoreactivity to p53, as did 5/9 of our GC-GBMs, as expected (Tables 1, 2). All E-GBMs showed uniform retention of BAF47 (INI-1) immunostaining throughout the tumor, in contrast to the R-GBMs in which focal loss was seen in both, as illustrated in our previous publication.[35] None of the de novo E-GBMs showed IDH-1 immunoreactivity; the sole case with IDH-1 immunoreactivity was the secondary E-GBM. Both R-GBMs showed low p53 immunostaining.

FISH Results

Genetic studies utilizing FISH revealed that 1 of 2 R-GBMs, 3 of 9 tested E-GBMs, and 2 of 4 tested GC-GBMs had *EGFR* amplification (Table 1). PTEN loss had predominantly been evaluated as part of the diagnostic workup in more recently diagnosed tumors, and of the 6 recent E-GBMs tested for PTEN loss, 2 were positive and 1 had low-level loss (Table 1). Thus, FISH results were not uniform within the *BRAF*-mutant E-GBM cohort and did not appear to show correlation with *BRAF* status (Table 1). The R-GBMs manifested monosomy 22. The sole secondary E-GBM arising from a mixed oligoastrocytoma was negative for loss of heterozygosity 1p, 19q (Table 1).

BRAF V600E Mutational Results in the Cohort

Four of the 5 new E-GBMs were positive for the *BRAF* V600E mutation (cases 11, 12, 14, and 15; Table 1). Three of our original E-GBMs were found in retrospect to possess the *BRAF* V600E mutation (cases 4, 7, and 10), and clues existed in the E-GBM of case 4 the features of which overlapped with that of PXA-A. Indeed, because of concern for PXA-A on our part, case 4 had been seen in consultation originally by neuropathologists at Mayo Clinic, Duke, and Johns Hopkins and diagnosed as "no definite pleomorphic xanthoastrocytoma component is present"; GBM with abundant reticulin; and malignant glioma with features of E-GBM.[35] Case 10 from our original study[35] had neuroimaging features suspicious for PXA-A with a cyst and mural nodule configuration (see Figs. 1E and F, from original paper).[35] However, it should be pointed out that other E-GBMs from our original cohort also showed unusual degrees of circumscription, dural attachment, or even cystic appearance[35] and were not found in this current study to possess the *BRAF* V600E mutation. While acknowledging that the small numbers of cases in the cohort precluded any meaningful statistical analysis or any definitive conclusions, our observation was that the *extent/scoring* of histologic features of E-GBMs—for example, how *extensive* the lymphocytic infiltrates or reticulin fibers were—did not reliably predict *BRAF* mutational status for any given tumor. In addition, TP53 IHC score and FISH results were not uniform within the *BRAF*-mutant E-GBM cohort (Table 1). TP53 IHC scores tended to be lower as a whole in E-GBMs than in GC-GBMs.

All R-GBMs and GC-GBMs showed an absence of *BRAF* V600E mutation, including the 2 pediatric GC-GBMs doubly assessed on frozen tumor DNA sample and after microdissection from a paraffin slide. Table 2 summarizes these *BRAF* results.

An electropherogram demonstrating a representative example of c.1799 T > A (p.V600E) mutation identified in case 11, with nucleotide and amino acid designations indicated, is provided as a representative example in Figure 3; other positive cases appeared identical on the electropherogram.

DISCUSSION

The current study demonstrates that a significant percentage (7/13 cases, 54%) of E-GBMs possess the *BRAF* V600E mutation. Although there are definitely areas of neuroimaging and histologic overlap between E-GBMs and PXA-As, there are also many differences. E-GBMs usually show complex neuroimaging features with multiple cysts and enhancing nodular tumor masses (Fig. 1), but some overlap with the simple cyst and mural nodule configuration of many PXAs[10] does exist (case 10,

FIGURE 2. A, E-GBMs were characterized by relatively monotonous sheets of small-sized to moderate-sized epithelioid cells with eosinophilic cytoplasm with rounded cell borders and a paucity of stellate cytoplasmic processes [case 14 illustrated; hematoxylin and eosin (H&E)]. B, At higher-power magnification, prominent nucleoli (arrow) and abundant eosinophilic cytoplasm could be seen, mimicking a rhabdoid phenotype (case 14 illustrated; H&E). C, Discohesive tumor cells could lead to areas almost identical to metastatic carcinoma or melanoma (case 12 illustrated; H&E). D, Variable numbers of accompanying non-neoplastic lymphocytes (arrow) add to the diagnostic overlap, at least focally, with metastatic carcinoma or melanoma (case 15 illustrated; H&E). E, E-GBMs in most cases showed almost complete cellular monotony (cases 11, 12, and 15), although slightly more variation in cellular size and scattered larger, sometimes multinucleated (arrow), cells could be identified (case 13 illustrated; H&E). F, Necrosis (arrow) was identified in 4 of 5 new E-GBMs (case 11 illustrated; H&E). G, Multiple mitotic figures (arrows) were found in all examples; note necrosis at higher magnification from this same patient at the left (case 11 illustrated; H&E). H, Strong diffuse S100 immunoreactivity (top) with more variable and patchy GFAP immunostaining (bottom) is characteristic of E-GBMs. Note spindled morphology of some cells on GFAP (arrows) (case 14 illustrated; IHC with light hematoxylin counterstain for S100 protein and glial fibrillary acidic protein). I, Foci with increased reticulin fiber deposition were often found in E-GBMs (case 15 illustrated; Gomori reticulum stain).

TABLE 2. Summary of Study Results

	Tumor Type	BAF47 (INI-1) IHC	p53 IHC Strongly Overexpressed (3+ or 4+ Immunostaining)	*BRAF* V600E Mutation Present
N = 13	E-GBMs	Retained in all tumor nuclei in all 13 cases	4 of 12 cases	7 of 13 cases
N = 9	GC-GBMs	Not done	5 of 9 cases	0 of 9 cases
N = 2	R-GBMs	Focally lost in nuclei of rhabdoid cells in 2 of 2 cases	0 of 2 cases	0 of 2 cases

p53 immunostaining (IHC) was estimated semiquantitatively, with a score of 0 for < 1%, 1+ given for 1% to 5%, 2+ for 6% to 25%, 3+ for 26% to 50%, and 4+ for > 50% of tumor cells showing immunoreactivity.

illustrated in our previous manuscript).[35] Histologically, PXA-As and E-GBMs often share features of dural attachment, lymphocytic infiltrates, and reticulin-rich areas, as shown in this study, but the absence of classic lower-grade PXA areas anywhere in E-GBMs, the relatively monotonous, epithelioid tumor morphology in large areas of E-GBMs but not PXA-As, and the absence of significant numbers of eosinophilic granular bodies in E-GBMs have led many pathologists and neuropathologists to diagnose E-GBMs as separate entities.[30–36]

The finding of *BRAF* V600E mutation in both E-GBMs and PXA-As does not prove that these tumors are identical, any more than finding that the common genetic *BRAF* V600E mutational background in PXA, WHO grade II, PXA-A, gangliogliomas, and extracerebellar pilocytic astrocytomas[1–3] proves that all these tumor types are equivalent to each other. Presence of a common genetic *BRAF* V600E mutational background also does not correlate with tumor grade, as PXA-As and E-GBMs are malignant gliomas, PXA is WHO grade II, and gangliogliomas and extracerebellar pilocytic astrocytomas are WHO grade I.

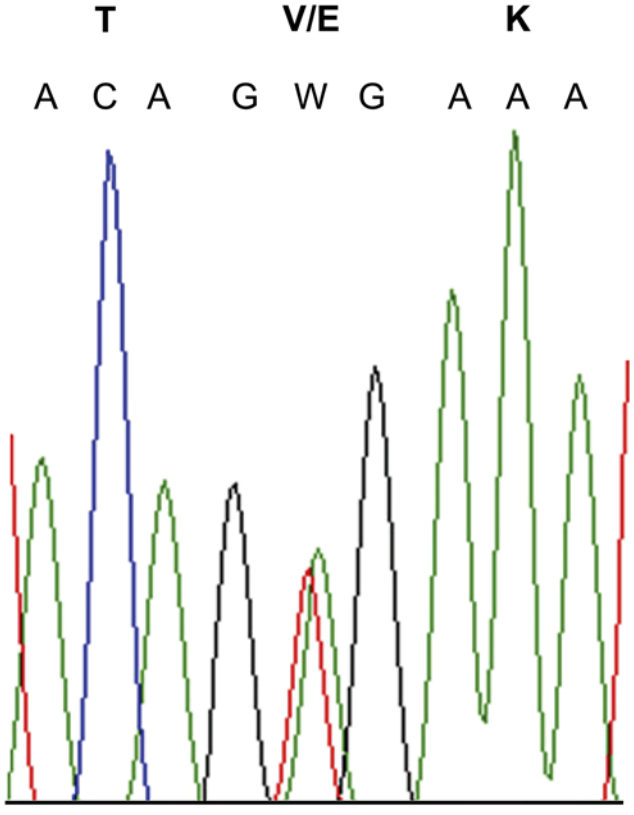

FIGURE 3. Electropherogram demonstrating a representative example of c.1799 T > A (p.V600E) mutation identified in 4 of 4 new E-GBM cases, with nucleotide and amino acid designations indicated (case 11 illustrated).

We were unable to identify a single "signature" demographic, neuroimaging, or histologic feature that was common to all *BRAF*-mutant E-GBMs that might obviate the need to perform *BRAF* mutational analysis testing. In addition, TP53 IHC score and FISH results were not uniform within the *BRAF*-mutant E-GBM cohort (Tables 1, 2). We noted, however, that the majority of GC-GBMs (5 of 9) and 1/3 of E-GBMs (4 of 12 assessed) showed strong 3+ or 4+ p53 IHC, whereas neither R-GBM showed this feature (Tables 1, 2). PXA-As may be histologically difficult to distinguish from either GC-GBMs or other types of GBMs.[28,2] When present, strong p53 IHC may be an additional feature that aids in the differential diagnosis of GC-GBM or E-GBM from PXA-A, as a significant percentage of both GC-GBMs and E-GBMs show strong p53 IHC expression, whereas only a minority of PXA-As strongly overexpress p53 by IHC[28] or show *TP53* mutation.[37]

We included GC-GBMs and R-GBMs for investigation of *BRAF* V600E mutational status. None of the cases in our cohort diagnosed as GC-GBMs or R-GBMs showed the mutation. We fully acknowledge that larger studies from other institutions will be necessary to verify our result in GC-GBMs. Given previous reports,[2,3] we anticipate that other groups may have a few GC-GBMs in their practice that do possess this mutation. However, it does not appear that GC-GBMs as a group are as significantly enriched for this mutation as are E-GBMs. It should also be noted that some studies show that up to 25% of GC-GBMs are mutated for *IDH-1*[4]; none of the GC-GBMs in our series were IDH-1 immunopositive. GC-GBMs could conceivably have heterogenous genetic origins.

It should also be emphasized that *absence* of *BRAF* mutation does not negate a histologic diagnosis of either PXA-A or E-GBM. Indeed, 100% of our E-GBMs did not show *BRAF* V600E mutation, neither did 100% of

PXAs or PXA-As, as reported in studies performed by several different groups worldwide using current WHO diagnostic criteria for these diagnoses.[1,2,3] Schindler et al[3] investigated a large number of PXAs (64: 38 adult, 26 pediatric) and PXA-As (23: 13 adult; 10 pediatric) and found the mutation in 66% of PXAs overall (63% adult, 69% pediatric) and 65% of PXA-As (38% adult, 100% pediatric). Dias-Santagata et al[2] found the mutation in 60% of WHO grade II PXAs but only in 17% of PXA-As, although a small number of the latter were assessed. On the basis of these studies from several different groups, at least one third of bona fide PXAs and PXA-As appear to be definitively negative for *BRAF* V600E mutation, and it is currently unclear whether 1, or more, as-yet-undiscovered genomic alterations might be present in this subset without *BRAF* V600E mutation. A similar percentage of E-GBMs in this study were also negative for *BRAF* V600E mutation.

In metastatic melanoma, the presence of *BRAF* mutation strongly correlates with young patient age, with all patients less than 30 years and only 25% of those at least 70 years of age having *BRAF*-mutant melanoma.[38] In the current study of E-GBMs, 5 of 7 E-GBM patients with *BRAF* V600E mutation were less than 30 years of age, although a 43-year-old man and a 50-year-old man with E-GBM each possessed *BRAF*-mutant tumor.

Testing for *BRAF* V600E mutational status may prove to be of more than passing academic interest in E-GBMs, PXAs, and PXA-As that require treatment in addition to surgical resection. Studies have shown the effectiveness and specificity of PLX4032 (vemurafenib), a Federal Drug Administration–approved kinase inhibitor used for targeted treatment of metastatic melanoma,[39,40] and suggested its potential use in the treatment of brain tumors harboring the *BRAF* V600E mutation.[41]

ACKNOWLEDGMENTS

The authors thank Diane Hutchinson for excellent manuscript preparation and Lisa Litzenberger for expert photographic assistance.

REFERENCES

1. Dougherty MJ, Santi M, Brose MS, et al. Activating mutations in *BRAF* characterize a spectrum of pediatric low-grade gliomas. *Neuro Oncol*. 2010;12:621–630.
2. Dias-Santagata D, Lam Q, Vernovsky K, et al. *BRAF* V600E mutations are common in pleomorphic xanthoastrocytoma: diagnostic and therapeutic implications. *PLoS One*. 2011;6:e17948.
3. Schindler G, Capper D, Meyer J, et al. Analysis of *BRAF* V600E mutation in 1320 nervous system tumors reveals high mutation frequencies in pleomorphic xanthoastrocytoma, ganglioglioma and extra-cerebellar pilocytic astrocytoma. *Acta Neuropathol*. 2011;121:397–405.
4. Balss J, Meyer J, Mueller W, et al. Analysis of the IDH1 codon 132 mutation in brain tumors. *Acta Neuropathol*. 2008;116:597–602.
5. Ichimura k, Pearson DM, Kocialkowski S, et al. IDH1 mutations are present in the majority of common adult gliomas but rare in primary glioblastomas. *Neuro Oncol*. 2009;11:341–347.
6. Capper D, Weissert S, Balss J, et al. Characterization of R132H mutation-specific IDH1 antibody binding in brain tumors. *Brain Pathol*. 2010;20:245–254.
7. Kepes JJ, Rubinstein LJ, Eng LF. Pleomorphic xanthoastrocytoma: a distinctive meningocerebral glioma of young subjects with relatively favorable prognosis. A study of 12 cases. *Cancer*. 1979;44:1839–1852.
8. Kepes JJ, Rubinstein LJ, Ansbacher L, et al. Histopathological features of recurrent pleomorphic xanthoastrocytomas: further corroboration of the glial nature of this neoplasm. A study of 3 cases. *Acta Neuropathol*. 1989;78:585–593.
9. Giannini C, Scheithauer BW, Burger PC, et al. Pleomorphic xanthoastrocytoma. *Cancer*. 1999;85:2033–2045.
10. Giannini C, Paulus W, Louis DN, et al. Pleomorphic xanthoastrocytoma. In: Louis DN, Ohgaki H, Wiestler OD, Cavenee WK, eds. *WHO Classification of Tumours of the Central Nervous System*. 3rd ed. Lyon: IARC; 2007:22–24.
11. MacKenzie JM. Pleomorphic xanthoastrocytoma in a 62-year-old male. *Neuropathol Appl Neurobiol*. 1987;13:481–487.
12. Marton E, Feletti A, Orvieto E, et al. Malignant progression in pleomorphic xanthoastrocytoma: personal experience and review of the literature. *J Neurol Sci*. 2007;252:144–153.
13. Kros JM, Vecht CJ, Stefanko SZ. The pleomorphic xanthoastrocytoma and its differential diagnosis: a study of five cases. *Hum Pathol*. 1991;22:1128–1135.
14. Chakrabarty A, Mitchell P, Bridges LR, et al. Malignant transformation in pleomorphic xanthoastrocytoma—a report of two cases. *Br J Neurosurg*. 1999;13:516–519.
15. Fu Y-J, Miyahara H, Uzuka T, et al. Intraventricular pleomorphic xanthoastrocytoma with anaplastic features. *Neuropathol*. 2010;30:443–448.
16. Ng WH, Lim T, Yeo TT. Pleomorphic xanthoastrocytoma in elderly patients may portend a poor prognosis. *J Clin Neurosci*. 2008;15:476–478.
17. Prayson RA, Morris HH 3rd. Anaplastic pleomorphic xanthoastrocytoma. *Arch Pathol Lab Med*. 1998;122:1082–1086.
18. Hirose T, Ishizawa K, Sugiyama K, et al. Pleomorphic xanthoastrocytoma: a comparative pathological study between conventional and anaplastic types. *Histopathology*. 2008;52:183–193.
19. Sugita Y, Shigemori M, Okamoto K, et al. Clinicopathological study of pleomorphic xanthoastrocytoma: correlation between histological features and prognosis. *Pathol Int*. 2000;50:703–708.
20. Tan T-C, Ho L-C, Yu C-P, et al. Pleomorphic xanthoastrocytoma: report of two cases and review of the prognostic factors. *J Clin Neurosci*. 2004;11:203–207.
21. Tekkök IH, Sav A. Anaplastic pleomorphic xanthoastrocytomas. Review of the literature with reference to malignancy potential. *Pediatr Neurosurg*. 2004;40:171–181.
22. Okazaki T, Kageji T, Matsuzaki K, et al. Primary anaplastic pleomorphic xanthoastrocytoma with widespread neuroaxis dissemination at diagnosis—a pediatric case report and review of the literature. *J Neurooncol*. 2009;94:431–437.
23. Vu TM, Liubinas SV, Gonzales M, et al. Malignant potential of pleomorphic xanthoastrocytoma. *J Clin Neurosci*. 2012;19:12–20.
24. Korshunov A, Golanov A. Pleomorphic xanthoastrocytomas: immunohistochemistry, grading and clinico-pathologic correlations. An analysis of 34 cases from a single Institute. *J Neurooncol*. 2001;52:63–72.
25. Macaulay RJ, Jay V, Hoffman HJ, et al. Increased mitotic activity as a negative prognostic indicator in pleomorphic xanthoastrocytoma. Case report. *J Neurosurg*. 1993;79:761–768.
26. Pahapill PA, Ramsay DA, Del Maestro RF. Pleomorphic xanthoastrocytoma: case report and analysis of the literature concerning the efficacy of resection and the significance of necrosis. *Neurosurgery*. 1996;38:822–829.
27. Kleihues P, Burger PC, Aldape KD, et al. Glioblastoma. In: Louis DN, Ohgaki H, Wiestler OD, Cavenee WK, eds. *WHO Classification of Tumours of the Central Nervous System*. Albany, New York: WHO Publications Center; 2007:33–49.
28. Martinez-Diaz H, Kleinschmidt-DeMasters BK, Powell SZ, et al. Giant cell glioblastoma and pleomorphic xanthoastrocytoma show different immunohistochemical profiles for neuronal antigens and p53 but share reactivity for class III beta-tubulin. *Arch Pathol Lab Med*. 2003;127:1187–1191.

29. Watanabe K, Sato K, Biernat W, et al. Incidence and timing of p53 mutations during astrocytoma progression in patients with multiple biopsies. *Clin Cancer Res*. 1997;3:523–530.
30. Rosenblum MK, Erlandson RA, Budzilovich GN. The lipid-rich epithelioid glioblastoma. *Am J Surg Pathol*. 1991;15:925–934.
31. Fuller GN, Goodman JC, Vogel H, et al. Epithelioid glioblastoma: a distinct clinicopathologic entity. *J Neuropathol Exp Neurol*. 1998;57:501.
32. Akimoto J, Namatame H, Haraoka J, et al. Epithelioid glioblastoma: a case report. *Brain Tumor Pathol*. 2006;22:21–27.
33. Rodriguez FJ, Scheithauer BW, Giannini C, et al. Epithelial and pseudoepithelial differentiation in glioblastoma and gliosarcoma: a comparative morphologic and molecular genetic study. *Cancer*. 2008;113:2779–2789.
34. Gasco J, Franklin B, Fuller GN, et al. Multifocal epithelioid glioblastoma mimicking cerebral metastasis: case report. *Neurocirugia (Astur)*. 2009;20:550–554.
35. Kleinschmidt-DeMasters BK, Alassiri AH, Birks DK, et al. Epithelioid versus rhabdoid glioblastomas are distinguished by monosomy 22 and immunohistochemical expression of INI-1 but not Claudin 6. *Am J Surg Pathol*. 2010;34:341–354.
36. Tanaka S, Nakada M, Hayashi Y, et al. Epithelioid glioblastoma changed to typical glioblastoma: the methylation status of MGMT promoter and 5-ALA fluorescence. *Brain Tumor Pathol*. 2011;28:59–64.
37. Kaulich K, Blaschke B, Nümann A, et al. Genetic alterations commonly found in diffusely infiltrating cerebral gliomas are rare or absent in pleomorphic xanthoastrocytomas. *J Neuropathol Exp Neurol*. 2002;61:1091–1099.
38. Menzies AM, Haydu LE, Visintin L, et al. Distinguishing clinicopathologic features of patients with V600E and V600K *BRAF*-mutant metastatic melanoma. *Clin Cancer Res*. 2012;18:3242–3249.
39. Chapman PB, Hauschild A, Robert C, et al. Improved survival with vemurafenib in melanoma with *BRAF* V600E mutation. *N Engl J Med*. 2011;364:2507–2516.
40. Sosman JA, Kim KB, Schuchter L, et al. Survival in *BRAF* V600-mutant advanced melanoma treated with vemurafenib. *N Engl J Med*. 2012;366:707–714.
41. Nicolaides TP, Li H, Solomon DA, et al. Targeted therapy for *BRAF*V600E malignant astrocytoma. *Clin Cancer Res*. 2011;17:7595–7604.